

citation. This is further supported by the observation that the position of the lower energy peak coincides approximately with that observed in the electron impact $P(\epsilon)$ distribution (Figure 7a,b). In the 1.5- and 2-keV collision energy experiments, the $P(\epsilon)$ distributions no longer display structured profiles. This is probably due to the increased contribution of vibrational excitation at lower collision energies. Thus, activation of the parent ion by means of a vibrational mechanism is favored (i) by increasing the scattering angle and (ii) by decreasing the ion collision energy. A complete interpretation of the shapes of the $P(\epsilon)$ distributions remains difficult though. For example, at higher collision energies (7 keV) the zero-angle CAD experiment begins to show a bimodal structure (Figure 7c), perhaps because the zero-angle experiment includes off-axis contributions which, in combination with the large value of E , give $E\theta$ a significant value.

Conclusion

The internal energy deposited in $\text{Fe}(\text{CO})_5^{*+}$ and $\text{W}(\text{CO})_6^{*+}$ ions increases as the scattering angle at which products are collected is raised. The average energy transferred also varies with collision energy, increasing monotonically with the scattering parameter, $E\theta$. The internal energy distributions associated with these kiloelectron volt energy collision processes show structure at larger

values of $E\theta$. This structure is compared with that seen in electron impact and with the unstructured curves observed in low-energy ion/surface and gaseous collisions. These comparisons suggest that the major contribution to collision-induced dissociation in ARMS experiments in the keV energy range is made by vibrational excitation. The smaller, lower energy deposition component observed under some conditions is apparently due to simple electronic excitation. This latter conclusion must be recognized as tentative only; a significant alternative is that oblique collisions contribute to collisional activation. Much more needs to be learned about collisional dynamics before the second mechanism can be evaluated in more detail.

Acknowledgment. This work was supported by the National Science Foundation (CHE 87-21768).

Registry No. He, 7440-59-7; Ar, 7440-37-1; C_9F_{20} , 50285-18-2; $\text{Fe}(\text{CO})_5^+$, 59699-78-4; $\text{W}(\text{CO})_6^+$, 112908-02-8.

Supplementary Material Available: Figures showing internal energy distributions for $\text{Fe}(\text{CO})_5^{*+}$ at 3.0 keV and $\text{W}(\text{CO})_6^{*+}$ at 1.5 keV and tables of normalized daughter spectra (9 pages). Ordering information is given on any current masthead page.

Photoinduced Charge Separation in a Porphyrin–Tetraviologen Supramolecular Array

James D. Batteas,[†] Anthony Harriman,^{*†} Yu Kanda,[†] Noboru Mataga,^{*†} and Andreas K. Nowak[‡]

Contribution from the Center for Fast Kinetics Research, University of Texas at Austin, Austin, Texas 78712, Department of Chemistry, Faculty of Engineering Science, Osaka University, Toyonaka, 560 Osaka, Japan, and Davy Faraday Research Laboratory, The Royal Institution, 21 Albemarle Street, London W1X 4BS, U.K. Received March 3, 1989

Abstract: A porphyrin–tetraviologen supramolecule P–V₄, in which a viologen molecule is appended to each of the porphyrin meso positions via a 1,3-propanoxy-4-phenyl chain, has been studied by picosecond and nanosecond laser flash photolysis techniques. In DMSO solution, rapid charge separation (CS) occurs from the first excited singlet state of the porphyrin, giving rise to long-lived redox products. These products recombine via first-order kinetics ($\tau = 6.4 \pm 0.7 \mu\text{s}$) to restore the ground-state reactants. Similar, but much slower, CS takes place from the porphyrin triplet excited state, which is formed in competition to CS from the singlet state. Quantum yields for formation of redox products and rates of both CS and charge recombination (CR) are solvent dependent, protic solvents favoring rapid CR.

There is much current interest in the design and study of molecular models capable of mimicking the rapid electron-transfer processes that occur in photosynthetic reaction center complexes.¹ Most models employ a chromophore covalently linked to an electron acceptor or donor via a flexible or rigid spacer group. In many cases, a porphyrin has been used as the chromophore and either a quinone,^{2–7} a viologen,^{8–12} or a similar electron affinic species¹³ functions as electron acceptor.¹⁴ With the use of time-resolved fluorescence spectroscopy and ultrafast flash photolysis techniques, rate constants for charge separation (CS) and charge recombination (CR) have been determined and, in several instances, related to fundamental properties of the system. The effects of solvent, mutual orientation, separation distance, exoergicity, and type of spacer group upon the rates of CS and CR are among the main parameters being investigated at present.^{2–14} In closely related studies, the factors affecting intramolecular energy transfer¹⁵ and charge-shift reactions¹⁶ are being monitored.

More elaborate models have been synthesized in which two different electron acceptors have been attached to a single

(1) (a) Harriman, A. *Energy Resources through Photochemistry and Catalysis* Gratzel, M. Ed.; Academic Press: New York, 1983; p 163. (b) Wasielewski, M. R. *Photochem. Photobiol.* **1988**, *47*, 923. (c) Connolly, J. S.; Bolton, J. R. *Photoinduced Electron Transfer. Part D. Applications*; Fox, M. A.; Chanon, M., Eds.; Elsevier: Amsterdam, 1988; p 303. (d) Mataga, N. *Photochemical Energy Conversion*; Norris, J. R., Meisel, D., Eds.; Elsevier: New York, 1989; p 32.

(2) (a) Kong, J. L. Y.; Loach, P. A. *J. Heterocycl. Chem.* **1980**, *17*, 737. (b) Kong, J. L. Y.; Spears, K. G.; Loach, P. A. *Photochem. Photobiol.* **1982**, *35*, 545.

(3) (a) Ho, T.-F.; McIntosh, A. R.; Bolton, J. R. *Nature (London)* **1980**, *254*, 86. (b) Slemiarczuk, A.; McIntosh, A. R.; Ho, T.-F.; Stillman, M. J.; Roach, K. J.; Weedon, A. C.; Bolton, J. R.; Connolly, J. S. *J. Am. Chem. Soc.* **1983**, *105*, 7224. (c) Schmidt, J. A.; McIntosh, A. R.; Weedon, A. C.; Bolton, J. R.; Connolly, J. S.; Hurley, J. K.; Wasielewski, M. R. *J. Am. Chem. Soc.* **1988**, *110*, 1733.

(4) (a) Nishitani, S.; Karata, N.; Sakata, Y.; Misumi, S.; Migita, M.; Okada, T.; Mataga, N. *Tetrahedron Lett.* **1981**, *22*, 2099. (b) Migita, M.; Okada, T.; Mataga, N.; Nishitani, S.; Karata, N.; Sakata, Y.; Misumi, S. *Chem. Phys. Lett.* **1981**, *84*, 263. (c) Mataga, N.; Karen, A.; Okada, T.; Nishitani, S.; Kurata, N.; Sakata, Y.; Misumi, S. *J. Phys. Chem.* **1984**, *88*, 5138.

[†]University of Texas at Austin.

[‡]Osaka University.

[§]The Royal Institution.

chromophore¹⁷ and in which both donor and acceptor moieties have been bound to a porphyrin.¹⁸ These systems permit sequential electron-transfer steps leading to long-distance CS. In order to mimic more closely the natural organisms, cofacial¹⁹ and adjacent²⁰ porphyrin dimers having appended quinones have been synthesized. With such systems, it is possible that excitation energy transfer precedes electron transfer. Synthetic arrays containing four²¹ and five²² porphyrins have been described and used to model the natural-light harvesting complexes.

It was shown previously⁸ that a covalently bound viologen molecule quenches the excited singlet and triplet states of a porphyrin in polar solvents. Both quenching processes are expected to involve net electron transfer from the porphyrin to the appended viologen, but in most cases, only modest fluorescence quenching has been observed so that the formation of redox products from the excited singlet state has not been demonstrated unambiguously.

(5) (a) Dalton, J.; Milgrom, L. R. *J. Chem. Soc., Chem. Commun.* **1979**, 609. (b) Netzel, T. L.; Bergkamp, M. A.; Chang, C. K.; Dalton, J. *J. Photochem.* **1981**, *15*, 451. (c) Harriman, A.; Hosie, J. *J. Photochem.* **1981**, *15*, 163. (d) Joran, A. D.; Leland, B. A.; Geller, G. G.; Hopfield, J. J.; Dervan, P. B. *J. Am. Chem. Soc.* **1984**, *106*, 6090.

(6) (a) Wasielewski, M. R.; Niemczyk, M. P. *J. Am. Chem. Soc.* **1984**, *106*, 5043. (b) Wasielewski, M. R.; Niemczyk, M. P.; Svec, W. A.; Pewitt, E. B. *J. Am. Chem. Soc.* **1985**, *107*, 1080. (c) Hofstra, U.; Schaafsma, T. J.; Sanders, G. M.; van Dijk, M.; van der Plas, H. C.; Johnson, D. G.; Wasielewski, M. R. *Chem. Phys.* **1988**, *151*, 169.

(7) (a) Lindsey, J. S.; Mauzerall, D. C.; Linschitz, H. *J. Am. Chem. Soc.* **1983**, *105*, 6528. (b) Lindsey, J. S.; Delaney, J. K.; Mauzerall, D. C.; Linschitz, H. *J. Am. Chem. Soc.* **1988**, *110*, 3610.

(8) (a) Harriman, A.; Porter, G.; Wilowska, A. *J. Chem. Soc., Faraday Trans. II* **1984**, *80*, 193. (b) Blondeel, G.; De Keukerleire, D.; Harriman, A.; Milgrom, L. R. *Chem. Phys. Lett.* **1985**, *118*, 77. Harriman, A. *Inorg. Chim. Acta* **1984**, *88*, 213.

(9) (a) Kanda, Y.; Sato, H.; Okada, T.; Mataga, N. *Chem. Phys. Lett.* **1986**, *129*, 306. (b) Saito, T.; Hirata, Y.; Sato, H.; Yoshida, T.; Mataga, N. *Bull. Chem. Soc. Jpn.* **1988**, *61*, 1925.

(10) (a) McMahon, R. J.; Force, R. K.; Patterson, H. H.; Wrighton, M. S. *J. Am. Chem. Soc.* **1988**, *110*, 2670. (b) Force, R. K.; McMahon, R. J.; Yu, J.; Wrighton, M. S. *Spectrochim. Acta, Part A*, in press.

(11) (a) Leighton, P.; Sanders, J. K. M. *J. Chem. Soc., Chem. Commun.* **1984**, 856. (b) Irvine, M. P.; Harrison, R. J.; Beddard, G. S.; Leighton, P.; Sanders, J. K. M. *Chem. Phys.* **1986**, *104*, 315.

(12) Nakamura, H.; Motonaga, A.; Ogata, T.; Nakao, S.; Nagamura, T.; Matsuo, T. *Chem. Lett.* **1986**, 1615.

(13) (a) Cowans, J. A.; Sanders, J. K. M.; Beddard, G. S.; Harrison, R. J. *J. Chem. Soc., Chem. Commun.* **1987**, 55. (b) Harrison, R. J.; Pearce, B.; Beddard, G. S.; Cowans, J. A.; Sanders, J. K. M. *Chem. Phys.* **1987**, *116*, 429. (c) Wasielewski, M. R.; Johnson, D. G.; Svec, W. A.; Kersey, K. M. *J. Am. Chem. Soc.* **1988**, *110*, 7219.

(14) For corresponding nonporphyrin-based systems see: (a) Mataga, N. *Pure Appl. Chem.* **1984**, *56*, 1255. (b) Mataga, N.; Mlyashi, H.; Asahi, T.; Ojima, S.; Okada, T. *Ultrafast Phenomena VI. Springer Ser. Chem. Phys.* **1988**, *48*, 511. (c) Verhoeven, J. W.; Paddon-Row, M. N.; Hush, N. S.; Oevering, H.; Heppener, M. *Pure Appl. Chem.* **1986**, *58*, 1265. (d) Warman, J. M.; de Haas, M. P.; Paddon-Row, M. N.; Cotsaris, E.; Hush, N. S.; Oevering, H.; Verhoeven, J. W. *Nature (London)* **1986**, *320*, 615. (e) Finckh, P.; Heitele, H.; Volk, M.; Michel-Beyerle, M. E. *J. Phys. Chem.* **1988**, *92*, 6584.

(15) (a) Closs, G. L.; Piotrowiak, P.; MacInnis, J. M.; Fleming, G. R. *J. Am. Chem. Soc.* **1988**, *110*, 2652. (b) Oevering, H.; Verhoeven, J. W.; Paddon-Row, M. N.; Cotsaris, E.; Hush, N. S. *Chem. Phys. Lett.* **1988**, *143*, 488.

(16) (a) Calcaterra, L. T.; Closs, G. L.; Miller, J. R. *J. Am. Chem. Soc.* **1983**, *105*, 670. (b) Miller, J. R.; Calcaterra, L. T.; Closs, G. L. *J. Am. Chem. Soc.* **1984**, *106*, 3047.

(17) (a) Nishitani, S.; Kurata, N.; Sakata, Y.; Misumi, S.; Karen, A.; Okada, T.; Mataga, N. *J. Am. Chem. Soc.* **1983**, *105*, 7771. (b) Gust, D.; Moore, T. A.; Moore, A. L.; Barrett, D.; Harding, L. O.; Makings, L. R.; Liddell, P. A.; De Schryver, F. C.; Van der Auweraer, M.; Bensasson, R. V.; Rougee, M. *J. Am. Chem. Soc.* **1988**, *110*, 321.

(18) (a) Moore, T. A.; Gust, D.; Mathis, P.; Mialocq, J. C.; Chachaty, C.; Bensasson, R. V.; Land, E. J.; Doizi, D.; Liddell, P. A.; Nemath, G. A.; Moore, A. L. *Nature (London)* **1984**, *307*, 630. (b) Gust, D.; Moore, T. A. *J. Photochem.* **1985**, *29*, 173.

(19) Sakata, Y.; Nishitani, S.; Nishimizu, N.; Misumi, S.; McIntosh, A. R.; Bolton, J. R.; Kanda, Y.; Karen, A.; Okada, T.; Mataga, N. *Tetrahedron Lett.* **1985**, *26*, 5207.

(20) (a) Sessler, J. L.; Johnson, M. R.; Lin, T.-Y.; Creager, S. E. *J. Am. Chem. Soc.* **1988**, *110*, 3659. (b) Gust, D.; Moore, T. A.; Moore, A. L.; Makings, L. R.; Seely, G. R.; Ma, X.; Trier, T. T.; Gao, F. *J. Am. Chem. Soc.* **1988**, *110*, 7567.

(21) Dubowchik, G. W.; Hamilton, A. D. *J. Chem. Soc., Chem. Commun.* **1986**, 1391.

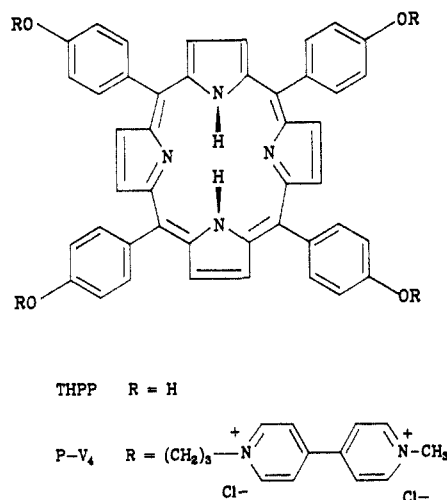
(22) Davila, J.; Harriman, A.; Milgrom, L. R. *Chem. Phys. Lett.* **1987**, *136*, 427.

With the reactants held in a face-to-face coplanar arrangement,¹¹ rapid CS and CR steps have been observed and, here, fluorescence quenching is extremely efficient. With more pliable structures,^{8,9} long-lived redox products have been detected but their origin remains unclear. Resonance Raman spectroscopy,¹⁰ following excitation of a P-V molecule with a 10-ns laser pulse, has confirmed the formation of CS products, the results being interpreted in terms of CS from the porphyrin singlet excited state. Other studies¹² with related P-V complexes have encountered problems with biphotonic and intermolecular processes that complicated analysis of the photophysical properties.

Attaching two viologens to a single porphyrin, P-V₂, ensures more efficient fluorescence quenching,⁹ overcoming some of the above experimental difficulties. In such cases, CS and CR occur on very fast time scales (i.e., 40 ps) for compounds with short (*n* = 3) connecting bridges. Much longer bridges appear to favor slower CS (i.e., 1 ns), but the CS products are relatively long-lived (i.e., hundreds of nanoseconds). Although picosecond flash photolysis studies^{9a} have suggested that CS occurs from the porphyrin excited singlet state, recent magnetic perturbation studies^{9b} have shown that they arise from the excited triplet state of the porphyrin. Increasing the number of attached viologens to four,^{8b} P-V₄, results in extremely efficient fluorescence quenching. Here, we describe experimental results showing that rapid CS from the excited singlet state of P-V₄ can give rise to a very long-lived (i.e., several microseconds) redox pair. Although CS and CR occur on very different time scales, the complex structure of this supramolecular array does not permit a detailed understanding of the actual pathways for the electron-transfer steps.

Experimental Section

meso-Tetrakis(4-hydroxyphenyl)porphyrin (THPP) was prepared and purified by conventional methods.²³ The corresponding tetraviologen derivative (P-V₄) was prepared and purified as before.^{8b,24,25} All synthesized compounds gave satisfactory elemental analyses, and all spectroscopic data were consistent with the assigned structures. Samples were further purified by TLC prior to the photophysical measurements. Methyl viologen was recrystallized from acetone, and all other materials were of the highest available purity and were used as received.



Absorption spectra were recorded with a Hewlett-Packard 8450A UV/Vis spectrophotometer, and fluorescence spectra were recorded with a Perkin-Elmer LS5 spectrofluorimeter after correction for instrumental responses.²⁶ Fluorescence quantum yields were determined relative to THPP ($\Phi_f = 0.12$),²⁷ and singlet excited-state lifetimes were measured by the single-photon counting technique, data analysis being made by the

(23) Bonnett, R.; Ioannou, S.; White, R. D.; Winfield, U.-J.; Berenbaum, M. C. *Photobiophys. Photobiophys. Suppl.* **1987**, 24.

(24) (a) Little, R. G.; Anton, J. A.; Loach, P. A.; Ibers, J. A. *J. Heterocycl. Chem.* **1975**, *12*, 343. (b) Little, R. G. *J. Heterocycl. Chem.* **1978**, *15*, 203.

(25) Milgrom, L. R. *J. Chem. Soc., Perkin Trans. I* **1983**, 2535.

(26) Argauer, R. J.; White, C. E. *Anal. Chem.* **1964**, *36*, 368.

(27) Bonnett, R.; McGarvey, D. J.; Harriman, A.; Land, E. J.; Truscott, T. G.; Winfield, U.-J. *Photochem. Photobiol.* **1988**, *48*, 271.

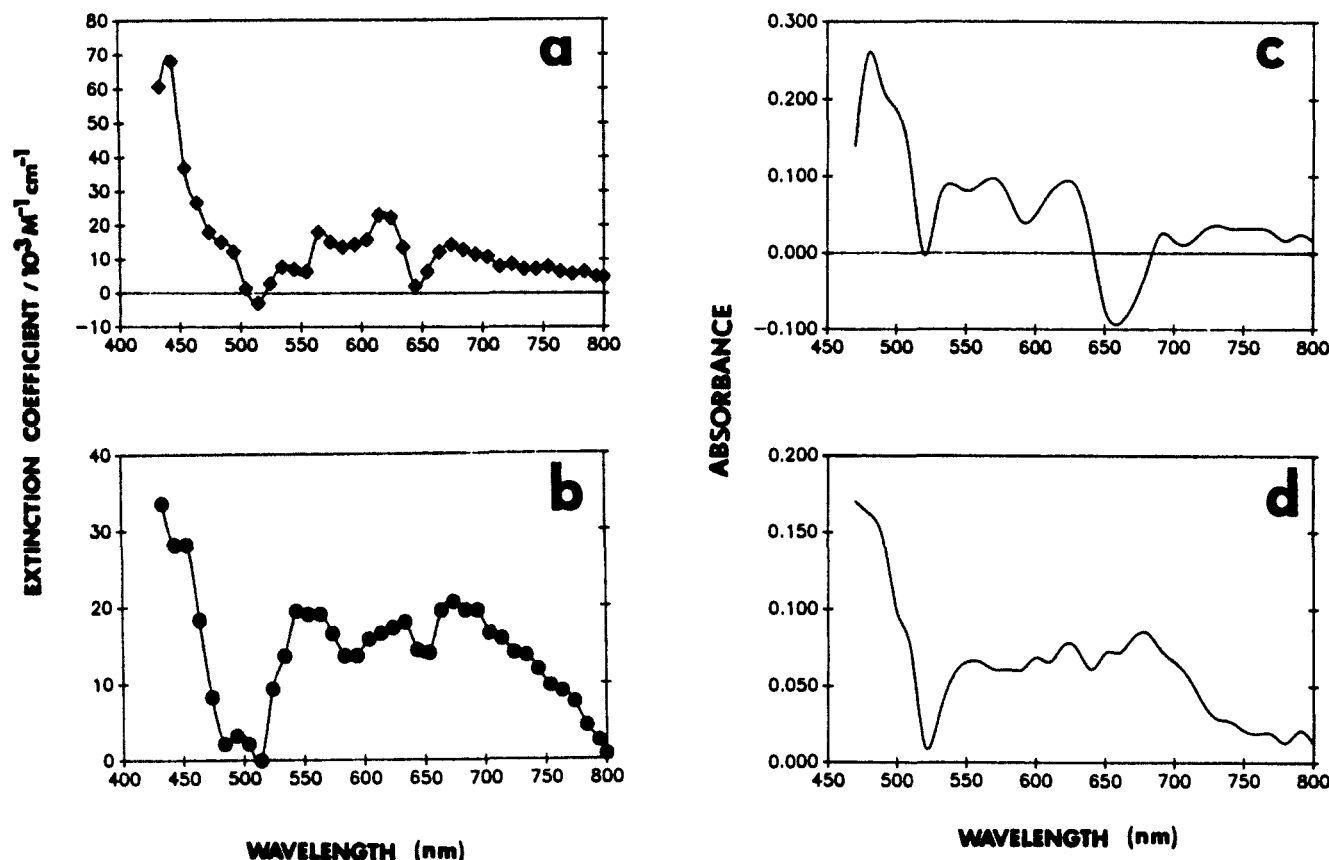


Figure 1. Transient absorption difference spectra recorded after excitation ($\lambda = 532$ nm) of THPP in N_2 -purged ethanol containing MV^{2+} . The spectra were recorded (a) 50 ns and (b) 10 μ s after excitation with a 10-ns laser pulse for $[MV^{2+}] = 1.5$ mM. With a 30-ps laser pulse and for $[MV^{2+}] = 0.42$ M, spectra were recorded (c) 50 ps and (d) 2 ns after excitation.

methods recommended by O'Connor and Phillips.²⁸ The excitation source for these studies was a synchronously pumped, cavity-dumped, mode-locked Nd:YAG dye laser. The time resolution of the instrument was 70 ps, and excitation was carried out at 590 nm. A high-radiance monochromator was used to isolate emitted photons in the wavelength range 660 ± 20 nm. For all fluorescence studies, air-equilibrated, optically dilute solutions were used.

Conventional flash photolysis studies were made with a frequency-doubled, Q-switched Nd:YAG laser as excitation source. Solutions were adjusted to possess an absorbance at 532 nm of ca. 0.2 and were purged with N_2 . Laser intensities were attenuated with crossed polarizers, and each determination was the average of about 50 individual laser shots. A frequency-doubled, mode-locked Nd:YAG laser was used for the picosecond flash photolysis studies, experiments being duplicated in Austin and Osaka with excellent agreement between the sets of data. Both instruments have been described in detail.²⁹ Laser intensities were calibrated with zinc tetraphenylporphyrin as standard, for which the triplet difference molar extinction coefficient³⁰ at 470 nm is $74\,000\text{ M}^{-1}\text{ cm}^{-1}$ and the triplet quantum yield³¹ is 0.83.

Cyclic voltammetry studies were made with a Rank E611 potentiostat driven by a purpose-built triangle wave generator. The solute (ca. 1 mM) was dissolved in an appropriate solvent containing tetra-*N*-butylammonium tetrafluoroborate (0.2 M) and purged thoroughly with N_2 . A Pt microelectrode was used as the working electrode, in conjunction with a Pt counter electrode and an SCE reference. In the reduction scans carried out with P-V₄, two quasi-reversible peaks could be resolved that corresponded to successive addition of electrons to the viologen moieties. The one-electron-reduction potential derived from such studies was solvent dependent; $E_{1/2}$ values of -0.19, -0.19, -0.20, -0.22, -0.35, and -0.44 V vs SCE, respectively, were found in *N,N*-dimethylformamide

(DMF), propylene carbonate (PC), dimethyl sulfoxide (DMSO), CH_3CN , CH_3OH , and water. Adsorption of the reduction product onto the electrode surface occurred, especially in water, and the above $E_{1/2}$ values have an expected accuracy of ± 30 mV. Redox potentials for one-electron oxidation of the porphyrin nucleus in P-V₄ were also solvent dependent; $E_{1/2}$ values of 1.11, 1.07, 1.05, 1.04, 0.82, and 0.78 V vs SCE, respectively, were obtained in DMF, PC, DMSO, CH_3CN , CH_3OH , and water. Again, there were problems with adsorption of the electrode-active species, and these derived values have an expected accuracy of ± 40 mV.

NMR studies were made in perdeuterated solvents with a GE 300 instrument by Fourier transform techniques. Spectra were accumulated at 295 K for approximately 0.1% solutions of P-V₄, and chemical shifts were determined relative to internal TMS. In DMSO-*d*₆ solution, it was confirmed that the observed chemical shifts were independent of P-V₄ concentration in the range of interest. However, in D_2O and CD_3OD solutions, the compound adsorbed onto the walls of the tube and the observed spectra were concentration dependent, presumably due to aggregation.

Molecular mechanics simulations on an isolated compound containing only one of the appended viologens were performed in the CHEM-X modeling program (Chemical Design Ltd., Oxford, U.K.). The calculations estimate the energy dependence of molecular conformations on both lengths and bond angles.³² The total energy of a conformation comprises terms for bond stretching, bond angle bending, changes in torsion angles, and nonbonded (van der Waals and coulombic) interactions. The program uses default functions and parameters following Allinger's MM2 program.³³ Four 180° bond rotations in the P-V molecule were performed, namely around the O-C₁, C₁-C₂, C₂-C₃, and C₃-N bonds in the connecting bridge, resulting in a total of 1296 different configurations.

Results and Discussion

Bimolecular Studies with Separated Molecules. In N_2 -purged ethanol solution, THPP exhibits modest fluorescence ($\Phi_f = 0.12 \pm 0.01$) and a reasonably long-lived excited singlet state ($\tau_s = 10.5 \pm 0.1$ ns).²⁷ Intersystem crossing to the triplet manifold

(28) O'Connor, D. V.; Phillips, D. *Time Correlated Single Photon Counting*; Academic Press: London, 1984.

(29) (a) Masuhara, H.; Ikeda, N.; Miyasaka, H.; Mataga, N. *J. Spectrosc. Soc. Jpn.* **1982**, *31*, 19. (b) Miyasaka, H.; Masuhara, H.; Mataga, N. *Laser Chem.* **1983**, *1*, 357. (c) Atherton, S. J.; Hubig, S. M.; Callen, T. J.; Duncanson, J. A.; Snowden, P. T.; Rodgers, M. A. J. *J. Phys. Chem.* **1987**, *91*, 3137.

(30) Pekkarinen, L.; Linschitz, H. *J. Am. Chem. Soc.* **1960**, *82*, 2407.

(31) Hurley, J. K.; Sinal, N.; Linschitz, H. *Photochem. Photobiol.* **1983**, *38*, 9.

(32) Burket, U.; Allinger, N. L. *ACS Monogr.* **1982**, *177*.

(33) Wertz, D. H.; Allinger, N. L. *Tetrahedron* **1974**, *30*, 1579.

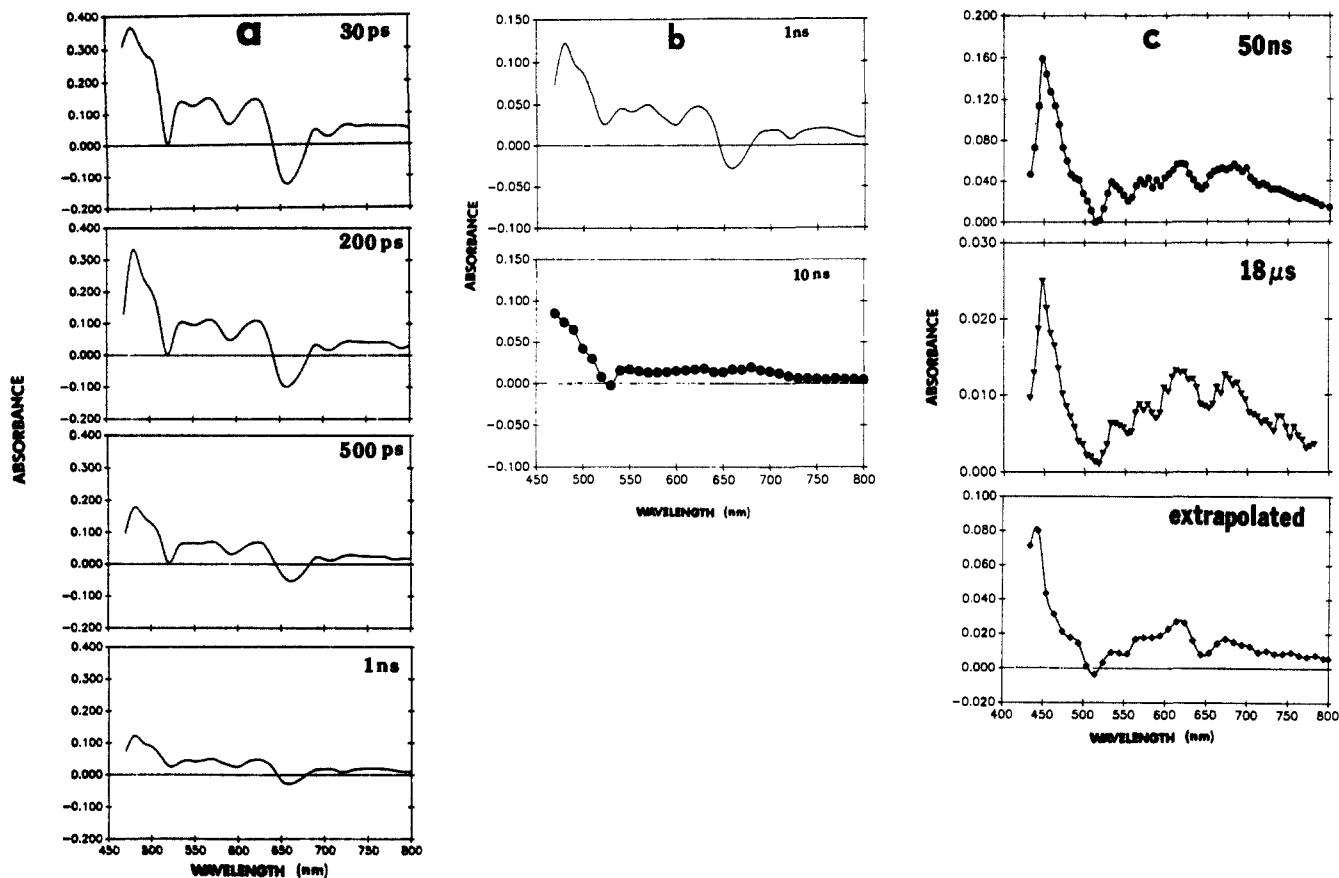


Figure 2. (a) Transient absorption difference spectra recorded various times after excitation ($\lambda = 532$ nm) of P-V₄ in N₂-purged DMSO solution with a 30-ps laser pulse. (b) Comparison of the transient absorption difference spectra recorded 1 and 10 ns after laser excitation; conditions as for Figure 2a. (c) Transient absorption difference spectra recorded 50 ns (●) and 18 μ s (▼) after excitation ($\lambda = 532$ nm) of P-V₄ in N₂-purged DMSO solution with a 10-ns laser pulse. The initial transient absorbance decayed via two competing first-order processes. Decay profiles were recorded for each wavelength and analyzed as the sum of two first-order reactions, and each initial absorbance was extrapolated to the center of the laser pulse. The longer lived transient spectrum so derived was equivalent to that recorded 18 μ s (▼) after the laser pulse and the shorter lived transient spectrum is shown separately (◆).

occurs with high efficiency ($\Phi_t = 0.65 \pm 0.06$), the lowest triplet state being long-lived ($\tau_t = 120 \pm 10 \mu$ s). Methyl viologen (MV²⁺) quenches both the excited singlet ($k_s = (4.4 \pm 0.3) \times 10^9 \text{ M}^{-1} \text{ s}^{-1}$) and triplet ($k_t = (2.0 \pm 0.2) \times 10^9 \text{ M}^{-1} \text{ s}^{-1}$) states of THPP under these conditions, although there was no indication of ground-state complexation. Flash photolysis experiments carried out in the absence of MV²⁺ allowed transient absorption spectra to be recorded for the porphyrin excited singlet and triplet states. In the presence of MV²⁺ (ca. 1 mM), such that the porphyrin singlet state is not quenched but almost quantitative quenching of the triplet state occurs, the characteristic absorption spectrum³⁰ of the porphyrin triplet state can be observed immediately after excitation with a 10-ns laser pulse (Figure 1a). This species decays via a first-order process to give a residual species (Figure 1b) that decays via second-order kinetics. The absorption profile and decay kinetics of this longer lived transient are consistent with its assignment to separated redox ion products.^{8a}



The bimolecular recombination process ($k_2 = (3.1 \pm 0.4) \times 10^8 \text{ M}^{-1} \text{ s}^{-1}$) is restricted by electrostatic repulsion between the ions, and on the basis of known extinction coefficients,³⁴ the efficiency for CS from the triplet excited state was $45 \pm 5\%$.

At much higher concentrations of MV²⁺ (ca. 0.4 M), such that the porphyrin fluorescence yield is reduced by ca. 95%, the porphyrin excited singlet state can be observed immediately after excitation with a 30-ps laser pulse (Figure 1c). This species decays rapidly ($\tau_s \approx 0.6$ ns) to give a residual absorption spectrum (Figure 1d) closely resembling that assigned above to separated electron-transfer products. In this case, the efficiency of CS is less than 10%. Thus, geminate recombination is much faster for the singlet ion pair than for the corresponding triplet ion pair due to spin selection rules,³⁵ the rate of CS being the same in both cases.^{36,37} In related systems, net electron-transfer products were detected with pheophytin³⁸ as photosensitizer but not when zinc mesoporphyrin^{9b} was used.

From luminescence studies,²⁷ the excited singlet and triplet states of THPP in ethanol are located at 1.88 ± 0.02 and 1.42 ± 0.05 eV, respectively. Cyclic voltammetry performed in ethanol solution gave a redox potential for one-electron oxidation of THPP of 0.83 ± 0.04 V vs SCE, whereas the redox potential for one-electron reduction of MV²⁺ was found to be -0.57 ± 0.03 V vs SCE. Since both redox products are positively charged, there will be an electrostatic energy barrier³⁷ of ca. 0.06 eV for net electron transfer. Consequently, photoinduced electron transfer involves free energy changes³⁹ of -0.40 ± 0.09 and $+0.04 \pm 0.12$ eV, respectively, for the porphyrin excited singlet and triplet states.

(34) At 600 nm there is an isosbestic point for the ground-state porphyrin-porphyrin π -radical cation difference spectrum. At this wavelength, the molar extinction coefficient for the viologen π -radical cation is $13\,200 \text{ M}^{-1} \text{ cm}^{-1}$, as determined by pulse radiolysis: Neta, P.; Richoux, M.-C.; Harriman, A. *J. Chem. Soc., Faraday Trans. 2* **1985**, *81*, 1427. The porphyrin π -radical cation absorbs strongly at 685 nm ($\epsilon = 12\,200 \text{ M}^{-1} \text{ cm}^{-1}$), as measured by pulse radiolysis in aerated propan-2-ol/water/CCl₄, 75/20/5.

(35) Gouterman, M.; Holten, D. *Photochem. Photobiol.* **1977**, *25*, 85.

(36) Fuoss, R. M. *J. Am. Chem. Soc.* **1958**, *80*, 5059.

(37) Richoux, M.-C.; Harriman, A. *J. Chem. Soc., Faraday Trans. 1* **1982**, *78*, 1873.

(38) Holten, D.; Windsor, M. W.; Parson, W. W.; Gouterman, M. *Photochem. Photobiol.* **1978**, *28*, 951.

(39) Includes an electrostatic energy correction for formation of two positively charged redox ions within a solvent cage (see ref 37).

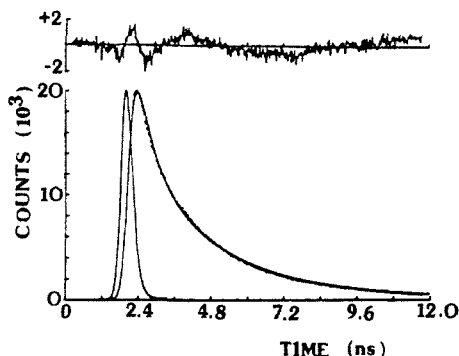


Figure 3. Fluorescence intensity decay profile recorded by the single-photon-counting technique following excitation ($\lambda = 590$ nm) of P-V₄ in air-equilibrated DMSO solution. After deconvolution of the instrument response function, the decay profile was analyzed as the sum of two exponential terms and the weighted residuals from this fit are shown at the top of the plot.

This calculation implies that the triplet (1.42 ± 0.05 eV) and the redox pair (1.46 ± 0.07 eV) are isoenergetic, but the spectroscopic studies show that the triplet decays via the redox pair.

Intramolecular Quenching by Appended Viologens. Attaching four viologens to the porphyrin ring, forming P-V₄,²⁵ has little effect on either the ground-state absorption or the fluorescence spectra in DMSO. Absorption spectra appear to be superimpositions of the individual spectra recorded for THPP and MV²⁺. Thus, the appended viologen groups do not perturb the ground or first excited singlet states of the porphyrin, and an absorption spectrum recorded 30 ps after excitation of P-V₄ in DMSO possessed the characteristic features of the porphyrin singlet excited state (Figure 2a). However, the fluorescence quantum yield for P-V₄ ($\Phi_f = 0.021 \pm 0.003$) was only 15% of that measured for THPP under identical conditions, showing that the terminal viologen groups function as efficient quenchers for the porphyrin excited singlet state.

The lifetime of the porphyrin first excited singlet state was measured by the time-correlated single-photon counting technique in dilute DMSO solution. Under identical conditions, fluorescence decay profiles recorded for THPP could be analyzed satisfactorily in terms of single-exponential fits, reduced $\chi^2 = 1.12$ being obtained. Fluorescence decay profiles recorded for P-V₄ could not be fit to a single-exponential process ($\chi^2 = 4.12$). Significantly better,²⁸ but far from ideal, fits to the sum of two-exponential terms were obtained ($\chi^2 = 1.40$). Fitting the data to the sum of three exponential terms did not really improve the quality of the fit ($\chi^2 = 1.32$) nor did analyzing the decay profile in terms of a Gaussian distribution of first-order rate constants about some mean value⁴⁰ ($\chi^2 = 3.77$). Fitting the decay profiles to the sum of two exponentials

$$I_f(t) = A_1 \exp(-t/\tau_1) + A_2 \exp(-t/\tau_2) \quad (3)$$

resulted in lifetimes of 0.62 and 2.83 ns with relative amplitudes of 54 and 46%, respectively (Figure 3). Quite similar values were obtained in Austin and in Osaka and with different samples of P-V₄, indicating that the multiexponential behavior does not result from instrumental artifacts or from impurities. It is necessary to consider, therefore, that there are at least two fluorescing species associated with P-V₄ in DMSO. A similar effect was found previously^{29a} for a porphyrin having two appended viologen molecules in acetone/methanol 1/1, but in DMSO, this same compound appeared as only one fluorescing species. Similarly, with porphyrins possessing only one appended viologen, the fluorescence decay profiles could only be analyzed in terms of multiexponential behavior.⁴¹

As shown in Figure 2a, picosecond flash photolysis studies indicate that the porphyrin excited singlet state can be detected

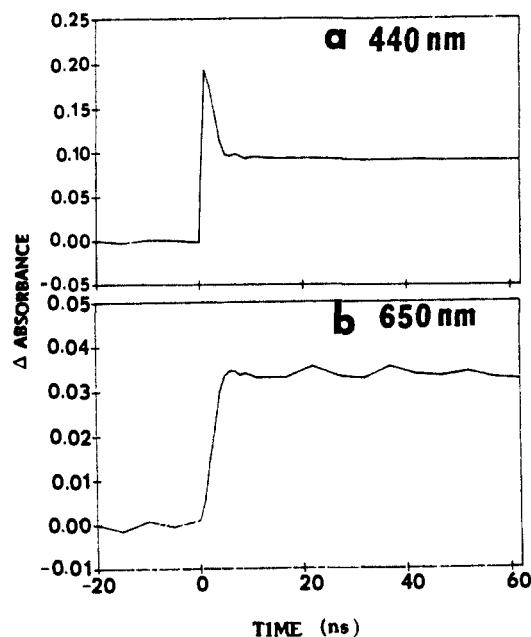


Figure 4. Absorbance changes observed at (a) 440 and (b) 650 nm following excitation ($\lambda = 532$ nm) of P-V₄ in N₂-purged DMSO solution with a 30 ps-laser pulse.

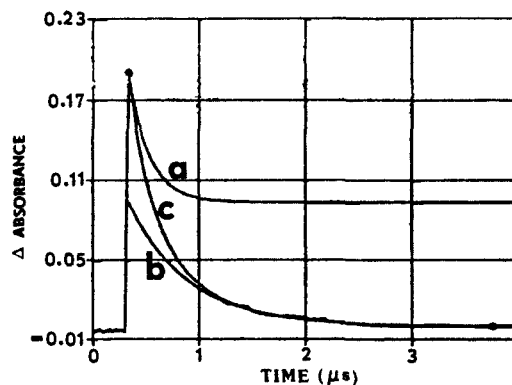


Figure 5. Absorbance changes observed at 460 nm following excitation ($\lambda = 532$ nm) of P-V₄ in N₂-purged DMSO solution with a 10-ns laser pulse. The decay profile has been analyzed as two competing first-order processes, giving lifetimes of (a) 2.2 and (b) 6.4 μ s. Trace (c) shows the actual decay profile and the computed fit.

immediately after excitation of P-V₄ in DMSO. The absorption decreases by approximately 50% during the first 500 ps following the laser flash, but the absorption profile remains essentially unchanged. A further decrease in absorbance occurs over the next 5 ns to leave a residual absorbance; a kinetic trace showing this effect is given in Figure 4a for $\lambda = 440$ nm where the porphyrin singlet excited state absorbs strongly. This residual absorption spectrum (Figure 2b) differs significantly from that observed immediately after the laser pulse (Figure 2a). Excitation with a 10-ns laser pulse gave an absorption spectrum very similar to that found at the end of the picosecond records (Figure 2c). This latter species decayed slowly; the actual decay profile was wavelength dependent and could only be analyzed in terms of two competing first-order processes (Figure 5). The shorter lived species decayed with a lifetime of 2.2 ± 0.2 μ s, whereas the longer lived species had a lifetime of 6.4 ± 0.7 μ s.

An absorption spectrum recorded after decay (i.e., 18 μ s) of the shorter lived transient can be assigned to an equimolar mixture of the porphyrin and viologen π -radical cations (Figure 2c), as formed by net electron transfer. Analyzing the kinetic traces acquired between 430 and 800 nm in terms of two competing first-order processes (Figure 5) and extrapolating to the center of the laser pulse allowed compilation of a difference absorption spectrum for the shorter lived transient (Figure 2c). It is seen

(40) Albery, W. J.; Bartlett, P. N.; Wilde, C. P.; Darwent, J. R. *J. Am. Chem. Soc.* **1985**, *107*, 1854.

(41) Harriman, A.; Nowak, A. K. *Pure Appl. Chem.*, in press.

that this latter spectrum is characteristic of a porphyrin triplet excited state.^{30,31}

The triplet state absorbs principally at 430–470 nm, whereas the redox products absorb strongly in the 600–700 nm region (Figures 1a,c and 2c). Monitoring at 450 nm and using the molar extinction coefficient determined for THPP ($\epsilon = 68\,000\text{ M}^{-1}\text{ cm}^{-1}$), the quantum yield for formation of triplet P-V₄ was found to be 0.12 ± 0.03 . At this wavelength, the redox products absorb less strongly ($\epsilon = 28\,200\text{ M}^{-1}\text{ cm}^{-1}$) and the quantum yield⁴² for formation of CS products was determined to be 0.17 ± 0.05 . Similar measurements made in the 600–700 nm region, where the products absorb more strongly with respect to the porphyrin triplet (Figure 2c), resulted in an average quantum yield for formation of redox products of 0.15 ± 0.03 .

The picosecond flash photolysis records confirm that decay of the porphyrin excited singlet state is complete within a few nanoseconds of excitation. Concomitant with deactivation of the singlet state there is a growth in the transient absorbance at 650 nm (Figure 4b) attributable to formation of an equimolar mixture of porphyrin and viologen π -radical cations. The porphyrin triplet possesses minimal absorption at 650 nm such that the appearance of redox products within a few nanoseconds of excitation by a short laser pulse indicates that they originate from the porphyrin excited singlet state.

The flash photolysis records can be summarized as follows. The porphyrin singlet excited state decays via two routes: a fast process that is complete within 1 ns and a slower process occurring over a few nanoseconds. The fast process results in re-formation of the porphyrin ground state without involvement of any long-lived intermediate state. The slower process involves formation of redox products and competing intersystem crossing to the triplet manifold. The triplet decays over a few microseconds and is much shorter lived than the corresponding triplet of THPP, indicating that the appended viologen quenches the triplet⁴³ as well as the singlet state of the porphyrin. The redox ion products decay via a relatively slow first-order process, with a lifetime of $6.4 \pm 0.7\ \mu\text{s}$, to re-form the ground-state molecule. These various lifetimes were found to be independent of the concentration of P-V₄, at least up to ca. 10^{-4} M , and of the laser intensity, showing that only intramolecular, monophotonic processes are being observed.

Both time-resolved fluorescence and picosecond transient absorption studies indicate that for P-V₄ the porphyrin excited singlet state decays by complex kinetics. This behavior may be attributed to electron-transfer reactions occurring in different families of conformations of the molecule that do not equilibrate on the nanosecond time scale. The fast process could be attributed to electron transfer between proximal partners within a group of conformations in which the porphyrin and one of the appended viologens are held in close proximity since a short molecular separation distance would favor rapid CS, but unless the products could diffuse apart on a very fast time scale, rapid CR would follow. This is the exact situation found in coplanar face-to-face porphyrin-viologen complexes¹¹ and in P-V₂ complexes with short ($n = 3$) connecting chains.^{9a} In turn, the slower process could be associated with a group of conformations in which all of the four appended viologens are kept some distance away from the porphyrin molecule. Here, the rate of CS would be slower because of the increased separation distance, but CR would also be much slower. Such conformations would endow the reactants with a high degree of mobility and allow the redox products to migrate to a position at which the electrostatic repulsive force was reduced to a minimum.^{9a} This would further reduce the rate of CR.

The above hypothesis requires that electron transfer proceeds through intervening solvent molecules rather than through the

framework of the connecting bridge. Partial support for this mechanism comes from the observation that with the corresponding P-V complexes the rate of CS depends markedly upon the site of attachment of the connecting chain.⁴¹ Also, it is difficult to rationalize the large difference in rates of CS and CR if the major route for electron transfer is through-bond not through-space. In the absence of clear experimental evidence, however, it is not possible to distinguish the pathway for the electron-transfer processes and, on the basis of our results, we cannot exclude a through-bond mechanism. In this case, the heterogeneity of the system would have to arise from local environmental effects, such as ion-pairing with the chloride counterions.

Another factor regulating the rates of CS and CR concerns the relevant energy gaps. For P-V₄ in polar medium, the standard free energy change accompanying CS from the first excited singlet state is ca. -0.6 eV , whereas CR involves a free energy change of ca. -1.26 eV . The rate constant for CS could be fairly large (ca. 10^{10} – 10^{11} s^{-1}) at $\Delta G^\circ = -0.6\text{ eV}$ provided the tunneling matrix element is not too small, while assuming the same tunneling matrix element, the rate constant for CR could take a value of $>10^{11}\text{ s}^{-1}$ at $\Delta G^\circ = -1.26\text{ eV}$.⁴⁴ Therefore, the very fast CS followed by rapid CR is in accordance with this consideration,⁴⁴ but the relatively slow CS followed by very slow CR cannot be interpreted on the basis of the simple energy gap dependence even if we assume a much smaller tunneling matrix element. In this latter case, we attribute the slow rate of CR to the redox products adopting an extended conformation in order to minimize electrostatic repulsion.

Because of efficient singlet-state quenching, the porphyrin triplet state is formed only in low yield and, by necessity, it will be formed only for conformations in which the appended viologens are held relatively far apart.^{8a} Computer modeling estimated the maximum separation distance to be ca. 2.5 nm. The low thermodynamic driving force, calculated to be ca. -0.16 eV , together with the increased separation distance, ensures that triplet quenching will be relatively inefficient and, from the flash photolysis studies, the rate constant for intramolecular electron transfer is $5 \times 10^5\text{ s}^{-1}$. However, the inherent triplet-state lifetime is ca. 100 μs , for which the translational distance⁴⁵ over which a viologen molecule can be expected to diffuse is ca. 180 nm. This means that the extended conformation required for triplet-state formation can relax within the triplet lifetime, and the observed rate of CS probably refers to a multitude of separation distances.

Conformation of the Porphyrin-Tetraviologen Molecule. The above discussion relies upon the P-V₄ molecule adopting a series of conformations in which the porphyrin and viologen units are held at different separation distances. In similar cases, NMR spectroscopy has provided key information pertaining to the conformation of the molecular assembly^{46,47} but this was not so for P-V₄ in DMSO-*d*₆. With four viologens attached to each porphyrin nucleus, individual viologens are expected to be found in a wide distribution of positions such that preferred conformations could not be detected. Compared to THPP, the observed chemical shifts implied that the porphyrin and viologen moieties fell within their mutual deshielding zones. Thus, the existence of "closed" conformations capable of demonstrating rapid CS and CR is to be expected in such solutions, but the apparent averaging of the NMR spectra suggests that the structure is in dynamic equilibrium on the microsecond time scale.

Further information about the conformation of P-V₄ was sought from computer modeling; for simplicity only one of the appended viologens was considered and the role of the solvent was ignored. The calculations predicted the existence of a wide number of conformations differing only slightly in energy and orientation.

(42) Measurements were made at a variety of laser intensities with a 10-ns pulse ($\lambda = 532\text{ nm}$). The initial absorbance attributable to redox products was determined at a series of wavelengths by extrapolating the longer lived decay profile back to the center of the laser pulse.

(43) In principle, it should be possible to observe a growth in the absorbance at 650 nm corresponding to formation of redox products from the porphyrin triplet excited state. However, the similarity in absorption spectra and lifetimes prevented unambiguous identification of CS from the triplet state.

(44) Mataga, N.; Asahi, T.; Kanda, Y.; Okada, T.; Kakitani, T. *Chem. Phys. Lett.* **1988**, *127*, 249.

(45) Calculated from $D = (dt)^{1/2}$ where D is the translational distance, d is the diffusion coefficient of the viologen ($d = 3.2 \times 10^{-6}\text{ cm}^2\text{ s}^{-1}$), and t is the time allowed for the movement ($t = 10^{-4}\text{ s}$).

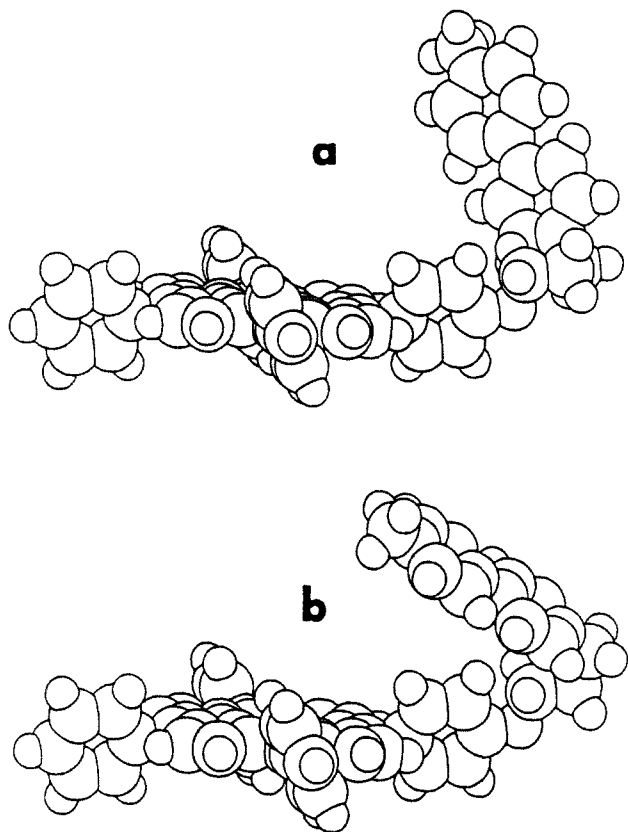
(46) Chachaty, C.; Gust, D.; Moore, T. A.; Nemath, G.; Liddell, P. A.; Moore, A. L. *Org. Magn. Reson.* **1984**, *22*, 39.

(47) Lisicki, M. A.; Mishra, P. K.; Bothner-By, A. A.; Lindsey, J. S. *J. Am. Chem. Soc.* **1988**, *110*, 3400.

Table I. Effect of Solvent on the Efficiency of CS and CR for P-V₄

solvent	ϵ^a	Φ^b (%)	τ_1 (ns)	τ_2 (ns)	A_1 (%)	τ_t (ns)	τ_{cr}^c (ns)	Φ_{cs}^d (%)
DMSO	46.7	84	0.52	2.8	54	2160	6400	33
DMF	36.7	81	0.55	3.7	51	470	2550	38
CH ₃ CN	37.5	91	0.37	1.9	64	132	315	8
PC	64.0	93	0.42	1.3	57	128	520	12
CH ₃ OH	32.6	95	0.20	1.1	71	240	35	5
H ₂ O	80.4	99	0.13	0.7	88	<i>e</i>	5	

^aBulk dielectric constant from ref 49. ^bFluorescence quenching efficiency $\Phi = [1 - (\Phi_f/\Phi_f^0)] \times 100\%$ where Φ_f and Φ_f^0 refer to the measured fluorescence quantum yields for P-V₄ and THPP, respectively. ^cLifetime for the redox products originating from the porphyrin excited singlet state. ^dQuantum efficiency for formation of CS products from the porphyrin excited singlet state. ^eNot observed.

**Figure 6.** Two most stable conformations computed for the porphyrin-mono viologen complex.

Rather surprisingly, the fully extended conformation was far from the most stable form,⁴⁸ and according to the calculations, this is not a preferred structure for P-V₄. The two most stable conformations are displayed in Figure 6. The preferred form (Figure 6a) has the viologen held almost perpendicular to the plane of the porphyrin ring. In this conformation, the center-to-center separation distance is ca. 1.52 nm. The second most stable conformation (Figure 6b) has a center-to-center separation distance of ca. 1.11 nm, and the viologen is held in an offset face-to-face orientation. These two forms are interconvertible by rotating the C₂-C₃ bond in the connecting bridge, for which the activation energy was computed to be ca. 45 kJ mol⁻¹.

The solvent, together with the presence of additional viologens appended to the porphyrin nucleus, will undoubtedly modify the above conformations. Despite such reservations about the validity of the computed structures, the spectroscopic data appear to be in accord with P-V₄ existing in families of conformations similar to those depicted in Figure 6. The rather closed conformation displayed in Figure 6b seems appropriate for the rapid CS and CR processes that account for about 50% of the porphyrin excited

singlet state. The less orthogonal and somewhat extended conformation shown in Figure 6a is consistent with the slower CS process that gives rise to long-lived redox products. This latter conformation has the facility for further extension to minimize electrostatic repulsion between the redox pair.

Solvent Effects. The photophysical properties of P-V₄ were determined, as above, in a range of polar solvents. In aprotic solvents, DMF, CH₃CN, and PC, the overall behavior was essentially identical with that described for DMSO solutions. Efficient fluorescence quenching was observed, and the complex fluorescence decay profiles had to be analyzed as the sum of two exponentials (Table I), both derived lifetimes being considerably shorter than the lifetime of THPP in that solvent. Flash photolysis studies indicated that the shorter lived species decayed rapidly to ground-state reactants without involvement of any long-lived intermediate state. The longer lived species observed in the fluorescence decay profiles decayed via formation of CS products and porphyrin triplet excited states. In all cases, the triplet lifetimes were quenched with respect to THPP (Table I), and their deactivation is expected to involve electron transfer to appended viologen. The rates of CS remained similar to that observed in DMSO although the overall efficiency of CS from the porphyrin excited singlet state decreased markedly upon changing the solvent from DMSO to CH₃CN or PC (Table I). Rates of CR and triplet decay varied considerably in the different solvents.

In CH₃OH solution, fluorescence quenching was extremely efficient and fluorescence decay profiles were dominated by the shorter lived component (Table I). Flash photolysis studies showed that CS products were produced on the time scale of a few nanoseconds, but the yield was low and CR was complete within 50 ns of excitation. The porphyrin triplet state, which was formed in very low yield ($\Phi_t \approx 0.04$), had a lifetime of only 240 ± 30 ns. Under these conditions, there was a small transient absorption remaining after decay of the triplet state, which had a lifetime of $1.8 \pm 0.4 \mu\text{s}$. This may be due to redox products arising from the triplet state, but because of its low concentration, it could not be demonstrated that it originated from a monophotonic process.

In water, fluorescence quenching is very efficient, with most (i.e., 90%) of the singlet excited state decaying within 200 ps. The residual singlet state decayed with a lifetime of 680 ps, which is very much shorter than found for THPP. Flash photolysis studies confirmed the rapid decay of the porphyrin singlet excited state; the characteristic features of the singlet disappeared within a few hundred picoseconds of excitation and gave rise to a transient spectrum resembling that assigned earlier to CS products. This redox pair decayed via complex kinetics with an average lifetime of 5 ± 2 ns. The porphyrin triplet state could not be detected in water ($\Phi_t < 0.03$), and ground-state P-V₄ was restored within 10 ns of excitation.

The experimental results obtained in the various polar solvents follow the general trend described for DMSO although the rates and yields of electron-transfer processes vary according to the nature of the solvent. In particular, the significance of the shorter lived component found in the fluorescence decay profiles increases in the protic solvents and induces a far greater degree of fluorescence quenching. Most probably, the solvent causes changes in the average conformational distribution, and on the assumption that these families of conformers do not equilibrate on the nanosecond time scale, this accounts for the different kinetic parameters given in Table I. Changes in solvent modulate things

(48) The computed energy gap between these conformers was only ca. 5 kJ mol⁻¹; the fully extended conformation was computed to be ca. 25 kJ mol⁻¹ less stable than the conformation shown in Figure 6a.

(49) Murov, S. L. *Handbook of Photochemistry*; Marcel Dekker: New York, 1973.

other than the molecular conformation, however, so that the observed solvent effects cannot be ascribed to any single factor. The thermodynamic driving forces, diffusion coefficients, and degree of ion-pairing will all be affected by solvent polarity and could contribute toward the observed rates of CS and CR.

Acknowledgment. We thank the SERC and the Japanese Ministry of Education, Science and Culture for financial support of this work. The Center for Fast Kinetics Research is supported jointly by the Biotechnology Research Resources Program of the NIH (Grant RR00886) and by the University of Texas at Austin.

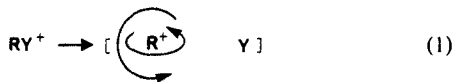
Internal Energy Effects on Ion-Neutral Complexes from Unimolecular Dissociation of *n*-Propyl Phenyl Ether Radical Cations

Eric L. Chronister and Thomas Hellman Morton*

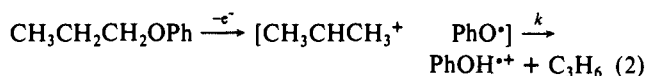
Contribution from the Department of Chemistry, University of California, Riverside, California 92521-0403. Received March 8, 1989

Abstract: The aliphatic portions of many alkyl phenyl ethers rearrange in the course of mass spectrometric fragmentation. Decomposition of the molecular ion of deuterated *n*-propyl phenyl ether has been examined in two energy regimes, near threshold by MIKES and at higher energy by resonant two-photon ionization followed by photodecomposition. Formation of phenol molecular ions is the predominant fragmentation pathway, and examination of *n*-propyl-2,2- d_2 (β - d_2) and *n*-propyl-1,1,3,3,3- d_5 (α,γ - d_5) phenyl ethers shows that the reaction proceeds via intermediate [isopropyl cation phenoxy radical] ion-neutral complexes in both regimes. In the photoionization/photodecomposition experiment the hydrogens within the isopropyl moiety become completely scrambled, while in the MIKES experiment decomposition of the ion-neutral complex via proton transfer occurs 3.7 times faster than scrambling of the alkyl hydrogens. A simplified density-of-states model is presented to describe the dependence of ion-neutral complex formation upon internal energy. Calculations based on this model give a qualitative result that agrees with experiment, namely that ion-neutral complex formation is more probable than simple bond fission.

An ion-neutral complex is a noncovalently bound aggregate of an ion with one or more neutral molecules. Such species are formed as transient intermediates in the unimolecular decomposition of a variety of gaseous ions, a subject that has been recently reviewed.¹ Because the highly directional nature of covalent or hydrogen bonding is absent, an ion-neutral complex possesses internal rotor degrees of freedom that do not exist in the covalently bound precursor. Equation 1 schematically depicts two of these internal degrees of freedom, bending vibrations of the R-Y bond of the covalent precursor RY⁺ that become internal rotations of the ion-neutral complex [R⁺ Y].



A series of experiments published in 1980 demonstrated that ion-neutral complexes are intermediates in the mass spectrometric decompositions of primary alkyl phenyl ethers.² This provided an explanation for several otherwise perplexing results. For instance, Benoit and Harrison had reported in 1976³ that molecular ions of *n*-propyl phenyl ether decompose to the phenol molecular ion and that the itinerant hydrogen comes from all three positions of the alkyl chain in nearly statistical proportions. The interpretation of this result in terms of an intermediate ion-neutral complex is shown in eq 2. Rapid scrambling of the hydrogens



in the isopropyl cation⁴ accounts for the indistinguishability of

the alkyl hydrogens prior to proton transfer to the phenoxy radical, a reaction that yields phenol^{H+} as the most prominent peak in the mass spectrum. Many alternatives have been ruled out, and eq 2 depicts a pathway for randomization of the alkyl hydrogens that is consistent with the distributions of hydrocarbon isomers expelled by larger alkyl phenyl ether molecular ions.

Lately a group at the Ecole Polytechnique has raised the question as to whether the mechanism of alkyl phenyl ether decompositions might change as a function of internal energy.⁵ Specifically, they suggest that elimination of phenol molecular ion via a six-member cyclic transition state, as represented schematically in eq 3, or a concerted hydrogen transfer from



carbon to oxygen could contribute a major pathway in some cases at very low internal energies. While it is entirely plausible that two mechanisms might compete with one another, we have presented arguments against there being a substantial change in mechanism as a function of internal energy.⁶

In order to probe this issue more deeply we report here the decomposition of deuterated analogues of *n*-propyl phenyl ether under two regimes. For a low-energy regime we have chosen to study metastable parent ions that live 10^{-6} s prior to fragmentation by using the MIKES (Metastable Ion Kinetic Energy Spectroscopy) technique on a reverse Nier-Johnson geometry mass spectrometer. Electron impact produces ions with a wide and, as yet, poorly defined distribution of internal energies. Only the

(1) McAdoo, D. J. *Mass Spectrometry Rev.* **1988**, *7*, 363-393.

(2) Morton, T. H. *J. Am. Chem. Soc.* **1980**, *102*, 1596-1602.

(3) Benoit, F. M.; Harrison, A. G. *Org. Mass Spectrom.* **1976**, *11*, 599-608.

(4) McAdoo, D. J.; McLafferty, F. W.; Bente, III, P. F. *J. Am. Chem. Soc.* **1972**, *94*, 2027-2033.

(5) Sozzi, G.; Audier, H. E.; Morgues, P.; Millet, A. *Org. Mass Spectrom.* **1987**, *22*, 746-747.

(6) Kondrat, R. W.; Morton, T. H. *Org. Mass Spectrom.* **1988**, *23*, 555-557.